CHEMBIOCHEM

DOI: 10.1002/cbic.200800739

Observing Proteins as Single Molecules Encapsulated in Surface-Tethered Polymeric Nanocontainers

Tobias Rosenkranz,[a] Alexandros Katranidis,[a, b] Diaa Atta,[a] Ingo Gregor,[c, f] Jörg Enderlein,[d] Mariusz Grzelakowski,[e] Per Rigler,[e] Wolfgang Meier,[e] and Jörg Fitter*[a]

Immobilizing biomolecules provides the advantage of observing them individually for extended time periods, which is impossible to accomplish for freely diffusing molecules in solution. In order to immobilize individual protein molecules, we encapsulated them in polymeric vesicles made of amphiphilic triblock copolymers and tethered the vesicles to a cover slide surface. A major goal of this study is to investigate polymeric vesicles with respect to their suitability for protein-folding studies. The fact that polymeric vesicles possess an extreme stability under various chemical conditions is supported by our observation that harsh unfolding conditions do not perturb the structural integrity of the vesicles. Moreover, polymerosomes prove to be permeable to GdnHCl and, thereby, ideally suited for unfolding and refolding studies with encapsulated proteins. We demonstrate this with encapsulated phosphoglycerate kinase, which was fluorescently labeled with Atto655, a dye that exhibits pronounced photoinduced electron transfer (PET) to a nearby tryptophan residue in the native state. Under unfolding conditions, PET was reduced, and we monitored alternating unfolding and refolding conditions for individual encapsulated proteins.

Introduction

Protein encapsulation in nanometer-sized cavities has become a frequently practiced technique that has been employed for a variety of applications in recent years. For example, protein encapsulation techniques are used for carrier-based drug delivery,[1–3] controlling and manipulating the protein microenvironment,[4–7] protecting proteins from denaturation and aggregation,[8,9] or for protein immobilization.[6,10–12] Besides encapsulation into sol–gel polymer matrices,[13] encapsulation into lipid vesicles[14,15] and polymeric vesicles[16,17] has been established. With respect to single-molecule studies, protein encapsulation is a key technique to immobilize water-soluble proteins within a native-like environment. In typical single-molecule studies using confocal microscopy, a tightly focused laser beam in combination with confocal detection defines a small volume out of which bursts of photons are collected from individual traversing proteins. Under these conditions, the observation time for a single protein is limited by the translational diffusion time of the molecule through the detection volume. However, a possibility of extended observation times ($>$ milliseconds) would allow one to monitor rare or slow dynamic events as well as repetitive processes with the same molecule. In order to achieve longer observation times, proteins need to be immobilized; optical or dielectrophoretic trapping techniques fail on a molecular level due to the low polarizabilities of individual molecules. One requirement for almost all single-molecules studies with immobilized proteins is to reduce, as much as possible, interactions of the protein with the surfaces of the enclosing cavity used for immobilization. In protein folding or during enzymatic action cycles, perturbing, protein-surface interactions might significantly alter the polypeptide structure and dynamics and can give rise to artifacts in the obtained results.[18] Several studies have demonstrated the successful confinement of proteins inside agarose gel matrices[19] or within lipid vesicles[6,20] without altering their structure and dynamics. Even anchoring proteins directly to a polymer-coated surface with a specific single-point attachment has given satisfactory results.[21] However, all these techniques have their advantages and disadvantages depending on the specific application.

Similar to lipid vesicles, vesicle-forming synthetic polymers have been recently employed as nanocontainers for encapsulating individual molecules. In particular, block copolymers have proven to be well-suited to forming vesicles in which proteins can be encapsulated.[16,17,22,23] With respect to protein-

[a] *T. Rosenkranz, A. Katranidis, D. Atta, Dr. J. Fitter*
Forschungszentrum Jülich, INB-2, Molecular Biophysics
52425 Jülich (Germany)
Fax: (+49) 2461-612020
E-mail: j.fitter@fz-juelich.de

[b] *A. Katranidis*
Laboratory of Biochemistry, School of Chemistry
Aristotle University of Thessaloniki
54124 Thessaloniki (Greece)

[c] *Dr. I. Gregor*
Forschungszentrum Jülich, INB-1, Cellular Biophysics
52425 Jülich (Germany)

[d] *Prof. J. Enderlein*
Institut für physikalische und theoretische Chemie
Eberhard Karls Universität Tübingen
72076 Tübingen (Germany)

[e] *Dr. M. Grzelakowski, Dr. P. Rigler, Prof. W. Meier*
Institut für Physikalische Chemie, Universität Basel
Klingelbergstrasse 80, 4056 Basel (Switzerland)

[f] *Dr. I. Gregor*
Present address: Forschungszentrum Caesar
Abteilung Molekulare Neurosensorik
Ludwig-Erhard-Allee 2, 53175 Bonn (Germany)

folding studies, vesicles from synthetic polymers (polymerosomes) offer several advantages. The vesicle preparation of polymerosomes in aqueous solution is easy and rather similar to procedures known for lipid vesicle formation. In contrast to lipid vesicles, however, polymerosomes are remarkably stable and remain structurally intact for months. In particular, their stability against structural disintegration at elevated temperatures, under osmotic and mechanical stress, or under other harsh environmental conditions has attracted attention.[17,24] In this study, we encapsulated proteins into polymerosomes and investigated the suitability of this system for studying protein folding on a single-molecule level. For this purpose, an ABA triblock copolymer with two hydrophilic blocks (A) and one hydrophobic block (B) was employed to form vesicles with a diameter in the range of 150–200 nm. During vesicle formation, we encapsulated fluorescently labeled proteins, namely PGK and BLA. The number of encapsulated proteins per vesicle and properties of the encapsulated proteins for different unfolding conditions have been analyzed. In the case of PGK, we followed unfolding and refolding transitions using PET between the fluorescent dye Atto655 and tryptophan residues, which are located in proximity in the protein structure (e.g., see refs. [25] and [26]).

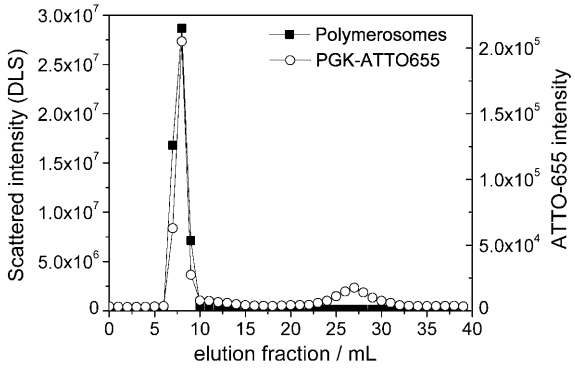

Figure 1. The elution profile shows that polymerosomes (measured by the intensity of scattered light) and the major amount of encapsulated protein (measured by fluorescence emission intensity) appear in the same elution fractions (6–10). A small fraction of nonencapsulated protein is visible in fractions 25–30. This profile corresponds to an initial protein concentration of 1 μM in the buffer during vesicle formation.

Results and Discussion

Protein encapsulation inside polymerosomes

To analyze the encapsulation efficiency during vesicle formation, we used buffers with free dye and with labeled proteins at different concentrations. A typical elution profile is shown in Figure 1. In this case, we observed high encapsulation efficiencies where most of the labeled PGK eluted together with the fraction that also contained polymerosomes. The encapsulation efficiency was rather similar for PGK and BLA and did not show a dependence on the type of attached dye. For higher initial protein concentrations (10 μM), the encapsulation efficiency was slightly smaller, as indicated by larger relative dye concentrations in elution fractions 25–30. From DLS, we obtained an average size of the polymerosomes in the 80–100 nm radius range with a rather narrow size distribution (see Figure 3D, below).

Since we did not know the absolute number of polymerosomes present in individual elution fractions, we could not directly estimate the number of encapsulated proteins per vesicle. However, this can be done with photobleaching measurements.[6,11,27] For this purpose, polymerosomes with encapsulated, fluorescently labeled proteins were immobilized on a glass surface and imaged with a wide-field microscope (see Figure 2A). After sufficiently extended illumination times, almost all the fluorophores attached to the proteins inside the vesicle will be photobleached. The number of encapsulated proteins can be estimated by the number of discrete photobleaching steps determined by abrupt drops in fluorescence intensity. Typical examples of the time course of step-wise, single-molecule photobleaching is shown in Figure 2 for one dye-labeled protein in a vesicle (Figure 2B), and for two proteins in a vesicle (Figure 2C). In principle, the process of protein encapsulation into vesicles follows Poisson statistics, yielding a probability distribution of numbers of proteins per vesicle (for details, see refs. [6] and [11]). With the lowest initial protein concentra-

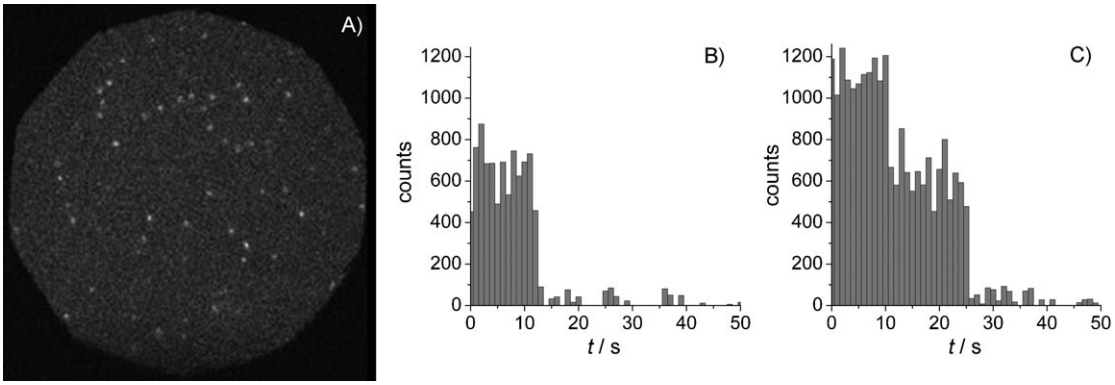

Figure 2. A) Wide-field fluorescence image of surface-tethered polymerosomes containing Atto655-labeled PGK. B) Single-step and C) two-step photobleaching events are presented, respectively, as time courses of fluorescence emission intensities, as obtained by integrating individual spots [data from the corresponding image (A) are shown].

tion used for encapsulation in this study (0.2 μM, see the Experimental Section), we observed that approximately 80% of all imaged polymerosomes exhibited one-step bleaching, and 20% exhibited two-step bleaching. According to the distribution statistics, we also expected to have a considerable fraction of polymerosomes with unlabeled proteins, but these will not show up in a fluorescence image. Hence, polymerosomes as prepared with our protocol are indeed suitable for single-molecule encapsulation. If not stated otherwise, we employed these polymerosomes containing on average one protein per vesicle for all subsequent measurements.

Characterizing folded and unfolded states of encapsulated proteins

A suitable encapsulation assay for protein-folding studies requires a durable and stable capsule. As known from numerous studies, vesicles made from triblock copolymers can ensure this kind of stability.[17,24] In most studies on protein folding, the unfolding process is initiated by either elevating the temperature (up to 60 °C) or by incubating the protein with high concentrations of denaturants such as urea or guanidine hydrochloride (GdnHCl). Earlier studies demonstrated that lipid vesicles can, in general, only partly withstand these conditions and start to disintegrate or become leaky after some time.[28] For lipid vesicles (made from EggPC, DMPC, and POPC), we observed in DLS measurements that the hydrodynamic radii and polydispersity increased at elevated temperatures (≈60 °C) and at higher concentrations (5 M) of GdnHCl. In contrast, our polymerosomes maintain their structure up to temperatures of at least 60 °C and GdnHCl concentrations of at least 5 M for hours. We observed no change in hydrodynamic radii (see Figure 3C) and the absence of any leakage under these conditions.[29] On the one hand, it is a prerequisite that the capsule is able to withstand protein unfolding conditions. On the other hand, it is also important that the unfolding conditions can affect proteins inside the vesicle. For temperature changes, this requirement is obviously met; heat dissipation easily takes place through the polymer membrane. Interestingly, the polymer membrane of our vesicles is permeable to GdnHCl, which offers the possibility to perform chemical unfolding/refolding studies on encapsulated proteins. In order to prove the GdnHCl permeability of the polymeric membrane, we made use of a specific dye property. In solution, Alexa633 exhibits a distinct redshift of the fluorescence emission spectrum upon transfer from native buffer conditions to a 5 M GdnHCl buffer (see Figure 3A). Polymerosomes with encapsulated dye, which were transferred from native buffer to different concentrations of GdnHCl in the buffer, show a similar spectral shift, slightly less pronounced for concentrations above 4 M (see Figure 3A and B). Therefore, we conclude that the membrane of our polymerosomes is permeable to GdnHCl. A 5 M GdnHCl concentration outside the polymerosomes leads to a spectral emission shift of the encapsulated dye that corresponds to a GdnHCl concentration of about 4 M, which is still sufficient to unfold PGK.[30] As demonstrated in Figure 3C and D, the transfer from native buffer conditions to highly concentrated GdnHCl buffer did not affect the structural integrity of the polymerosomes. To our knowledge, nothing is published about the permeability of liposomes to GdnHCl, but it is known from earlier studies that liposomes are permeable to urea.[31] In folding studies with proteins encapsulated in liposomes, a concentration of 2 M GdnHCl was applied to the vesicles.[20,32] This indicates that GdnHCl, at least at this concentration, seems not to initiate the disintegration of the liposomes.

For reasonable protein-folding studies we require undisturbed protein molecules that are freely diffusing inside the polymerosomes. Fluorescence polarization anisotropy provides valuable information in this respect. Using the technique, one can measure the rotational freedom of dyes bound to the pro-

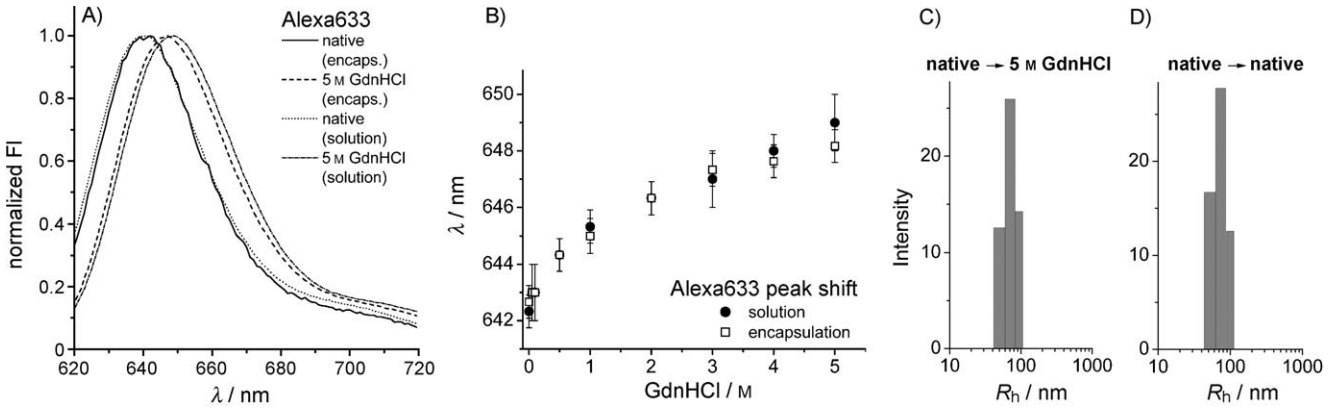

Figure 3. A) Normalized fluorescence emission spectra of unbound dye (Alexa633) are displayed for native buffer conditions and for 5 M GdnHCl buffer. The pronounced redshift (maximal shift 5–6 nm) is caused by the interaction of GdnHCl with the dye. Dyes were either freely diffusing in solution or encapsulated in polymerosomes. B) The spectral emission shift of Alexa633 in solution (solid symbols) and encapsulated in polymerosomes (open symbols) is shown as a function of GdnHCl concentration in the surrounding buffer. The GdnHCl-dependent shift is rather similar for free and encapsulated dye and proves at least a partial permeability of the vesicle membrane to GdnHCl. Fluorescence emission spectra were measured directly after the samples were incubated at the respective GdnHCl concentration. The observed peak positions did not change with time (that is, after 2–24 h), which indicates that the system was in equilibrium. The obtained values and the given standard deviations originate from three independent measurements. The size distributions of the polymerosomes, as obtained from DLS, are presented for C) polymerosomes transferred from native buffer to 5 M GdnHCl and for D) native buffer conditions. The almost identical size distributions for both buffer conditions indicate that the polymerosomes maintain their structural integrity upon GdnHCl treatment.

tein, and this allows one to detect potentially perturbing interactions of proteins with vesicle surfaces. In particular, unfolded proteins are often susceptible to such unwanted interactions. As visible from time-resolved and steady-state measurements (see Figure 4 and Table 1), unbound dyes, dyes bound to native proteins, and dyes bound to unfolded proteins exhibit different anisotropies. Time-resolved anisotropy decays (Figure 4) showed a fast and almost complete decay of the anisotropy within 2 ns for an unbound Atto655, which was indicative of a freely rotating molecule. In contrast, Atto655 bound to the native PGK exhibited a fast decay but thereafter reached a constant level of about 0.1. This indicated a partial rotational freedom of the bound dye, which was most probably confined within a groove on the protein surface. Whole-protein rotational motions are characterized by much longer correlation times of the order of 30 ns,[33] which are much longer than the Atto655 fluorescence lifetime ($\tau_f = 2$ ns). Therefore, we could not observe the complete anisotropy decay within the observation time of 10 ns. For unfolded PGK, the bound dye showed again a different behavior. We observed a slower but complete decay within the observation time. In this case, the dye seemed to experience a higher rotational freedom than did the native protein, because the protein structure had melted, and the formerly existing groove was no longer hindering rotational motion. Due to a rather flexible protein structure, local collisions could lead to a slower decay process. In contrast to the cases discussed so far, membrane-embedded dyes (Atto655-labeled DOPE molecule incorporated into the polymer matrix of the vesicles) revealed much weaker anisotropy decays with significantly larger final anisotropy values. Obviously, the dye attached to DOPE experienced a more pronounced rotational hindrance. In order to judge whether encapsulated proteins exhibit surface interactions or not, we compared the results from proteins in solution with those obtained from encapsulated proteins. This comparison revealed that anisotropy decays were rather similar for both cases (Figure 4). On the other hand, they differed significantly from values obtained for dyes more tightly coupled to the polymerosome (Atto655-labeled DOPE embedded in the polymer matrix). Within error limits, BLA and PGK exhibited similar results for dyes bound to the protein (Table 1). Therefore, we conclude that encapsulated proteins in the folded as well as in the unfolded state are not perturbed by interactions with polymerosome surfaces.

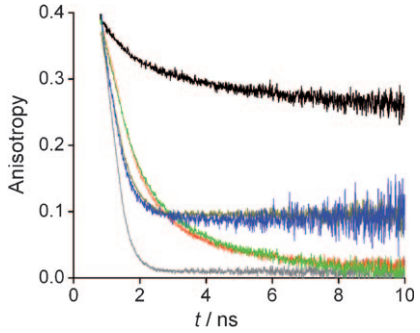

Figure 4. Anisotropy decays observed for Atto655 in the unbound state (gray curve), bound to freely diffusing native PGK (orange, almost hidden behind the blue curve), bound to freely diffusing unfolded PGK (red), and bound to polymer-matrix-embedded DOPE (black). Blue curves (native PGK) and green curves (unfolded PGK) represent measurements with encapsulated protein.

Table 1. Anisotropy values as obtained from steady-state measurements.

	Native buffer		5 M GdnHCl buffer	
	in solution	encapsulated	in solution	encapsulated
unbound Atto655	0.03 ± 0.002	0.04 ± 0.01	0.05 ± 0.002	–
PGK/BLA-Atto655[a]	0.12 ± 0.03	0.13 ± 0.05	0.09 ± 0.02	0.10 ± 0.05
DOPE-Atto655[b]	–	0.27 ± 0.02	–	–

[a] Anisotropy values for Atto655 bound to PGK or BLA are the same within the limits of error. [b] Atto655-labeled DOPE embedded in the polymer matrix of the polymerosome.

Application of PET to monitor the unfolding/refolding of PGK

For studying molecules on a single-molecule level, the ensemble techniques conventionally used for monitoring protein folding (for example, Trp fluorescence or CD spectroscopy) are not applicable due to poor sensitivity. To overcome this problem, the single-molecule fluorescence detection of dyes attached to the protein structure is usually employed.[18,34] Besides FRET and FCS studies, which essentially monitor the overall size and relative positions of specific sites in the protein structure for native and unfolded states,[32,35,36] a further technique, namely PET, was recently employed to follow protein-folding events.[26] In the case of PGK, we were able to make use of PET due to the fact that Atto655, attached at a defined position within the protein structure, is efficiently quenched by a Trp residue located in proximity to the dye. Upon unfolding, a structural expansion takes place, and the average distance between the dye and the quencher increases, which results in a lower quenching efficiency.[37] Although the native amino acid sequence of PGK contains a large number of lysine residues (target of the NHS-functionalized dyes), only two Lys residues (Lys213, Lys257) are in close proximity to the two Trp residues that are located in the C-terminal domain of the protein (see Figure 5A). A preferential labeling of these Lys residues would give us the opportunity to detect native (compact) and unfolded (expanded) states (at least of the C domain) by simply measuring the fluorescence emission intensity of Atto655. The results shown in Figure 5B indicate that a significant fraction of all the dyes bound to PGK is attached to one of these two favored Lys residues. As demonstrated in this figure, the thermally induced unfolding of the protein (monitored by intrinsic Trp fluorescence, blue lines) was accompanied by an increase of the Atto655 emission intensity (red lines), caused by reduced PET upon structural expansion during unfolding. A similar but much more pronounced increase in the emission intensity of Atto655 was observed for PGK incubated in 5 M GdnHCl buffer (see Figure 5C). This

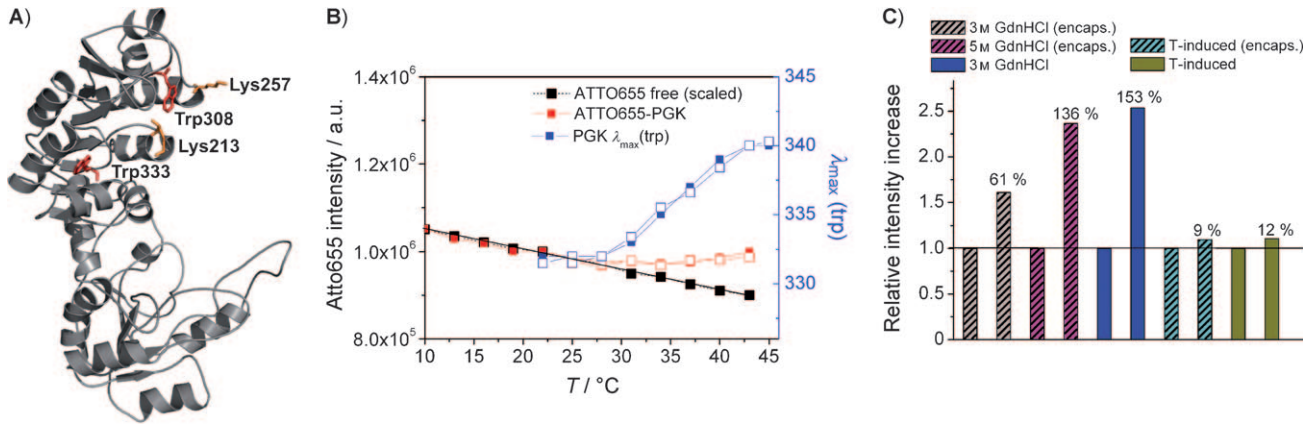

Figure 5. A) A structural model of PGK with highlighted Trp residues (red) and two nearby Lys residues (orange), which are putative binding sites for NHS-functionalized fluorescent dyes. B) For ensemble measurements in 0.7 M GdnHCl, 30 mM Mops, 50 mM NaCl, 2 mM EDTA, and pH 7.4, the reversible thermal unfolding of PGK was monitored by the shift of the Trp fluorescence emission peak (blue curves, right y-coordinate) and by the Atto655 emission intensity (red curves, left y-coordinate). In both cases, solid and open symbols represent data during heating and cooling, respectively. The black line represents the typical temperature dependence of the fluorescence intensity for free Atto655. The deviation of the red curves from the black curve at temperatures above 30 °C is caused by decreasing PET during spatial expansion of the unfolding PGK. The standard deviation for the experimental data points in this figure is on the order of the size of the symbols. C) For PGK in solution and encapsulated in polymerosmes, the relative Atto655 emission intensity is shown for various unfolding conditions. For native buffer conditions, the corresponding intensities were normalized to unity (see the horizontal line). Colored bars with stripes represent data from encapsulated protein (with approximately one protein/polymerosome).

much larger intensity increase is most probably due to the fact that GdnHCl also increases the dissociation constant of the non-fluorescent Trp-Atto655 complex.[37] As a consequence, GdnHCl alone reduces PET in steady-state measurements. Therefore, in contrast to temperature-induced unfolding, the much stronger signal increase in the Atto655 emission intensity observed for GdnHCl-induced unfolding is only partly caused by structural unfolding. Thus, for investigating unfolding conditions of polymerosome-encapsulated proteins on a single-molecule level, the GdnHCl-induced fluorescence intensity increase of Atto655 bound to PGK is a useful measure. In contrast to PGK, Atto655-labeled BLA did not show PET or a change in Atto655 fluorescence emission intensities upon protein unfolding. This indicates that for BLA, none of the Lys residues in the vicinity of Trp residues was labeled with Atto655. For all the proteins we labeled via multiple possible Lys residues (BLA, PGK, and additional α-amylases), we observed Atto655 fluorescence intensity changes caused by PET upon unfolding and refolding transitions only for PGK.

For single-molecule studies, surface-tethered polymerosomes containing encapsulated PGK were imaged with a closed imaging chamber. Images from samples incubated with native buffer and with 5 M GdnHCl buffer in an alternating sequence exhibit alternating intensity values from individual spots (Figure 6). For a large number of spots we observed an increase in intensities upon the change from native buffer to unfolding buffer conditions and a decrease in intensity when changing the buffer back to native conditions. This observation indicates that individual PGK molecules encapsulated in polymerosomes reversibly unfold or at least experience unfolding conditions upon incubation with 5 M GdnHCl buffer. To achieve more detailed information on the unfolded states of proteins or the characteristics of the unfolding/refolding transitions, which will be a task for our future studies, more elaborate approaches employing site-specific labeling are required. In particular, suitable cysteine mutants with dyes bound in close proximity to Trp residues can be used for more efficient, selective, Trp quenching.[26] In addition, proteins labeled at two defined position in the protein structure allow FRET measurements and can yield valuable structural information for different folding states.[12,20,32,35]

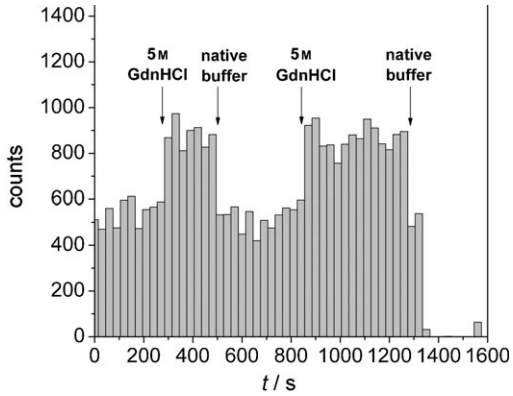

Figure 6. A typical time course of the measured emission intensity, as obtained from the integration of an individual spot, is shown in this figure. The images were measured every 30 s with polymerosomes bound to cover slides, which were built in a closed imaging chamber suitable for in situ buffer exchange. The arrows indicate buffer exchange from native to unfolding conditions or vice versa.

Conclusions

In this study, we have demonstrated that proteins encapsulated in polymeric vesicles offer the possibility to study individual proteins for extended time periods. The encapsulation procedure provides a native-like environment for water-soluble pro-

teins without any detectable hindrance from rotational reorientations. The high structural stability and considerable longevity of the polymerosomes qualifies them as an ideal tool for single-molecule studies. The permeability of triblock copolymer membranes to GdnHCl and their resistance against structural disintegration at high denaturant concentrations ensure ideal conditions for their use in protein-folding studies. At thermodynamic midtransition points (e.g. $GdnHCl_{1/2}$, $T_{1/2}$, $pH_{1/2}$) FRET-based approaches provide particularly good structural details during the folding and unfolding transitions of the proteins. Under these conditions, the folded and unfolded states have lifetimes of the order of seconds, and multiple, successive, unfolding/refolding transitions can be observed with FRET for single encapsulated proteins.[20,32] A major goal for future studies will be to focus on proteins that exhibit unfolding/folding transitions slow enough that trajectories of these transitions can be followed.[20] In addition, it was shown recently that channel proteins incorporated into the polymeric membrane can facilitate the transfer of solutes and substrates across the polymerosome membrane in a controlled manner,[7,38] similar to what has also been observed with liposomes.[12] In contrast to vesicles nonpermeant to substrates, channel-equipped polymeric nanocontainers allow for a much wider range of interesting applications. For instance, one can imagine studying conformational changes during catalysis or protein–substrate interactions using polymerosome-encapsulated proteins.

Experimental Section

Protein labeling: PGK from bakers yeast and BLA (both purchased from Sigma) were dissolved in sodium bicarbonate buffer (100 mM, pH 8.3). The proteins were purified using a PD10 desalting column (Sephadex G-25 matrix, GE Healthcare Bio-sciences). An NHS-ester functionalized dye (Atto655 from Atto-Tec, Siegen, Germany or Alex633 from Invitrogen) was added in threefold molar excess to a protein solution (5–10 μM protein) at room temperature. The mixture was incubated for 1 h, and free dye was removed with the Sephadex G-25 column. The labeling ratio was determined by using a calibration for which we measured the Trp fluorescence intensity as a function of protein concentration. With the known protein concentration of labeled proteins and with the measured dye concentration of labeled proteins from absorption spectroscopy (for Atto655, at 663 nm with $\varepsilon_{max} = 125\,000\ M^{-1}cm^{-1}$ and for Alexa633, at 630 nm with $\varepsilon_{max} = 164\,500\ M^{-1}cm^{-1}$), we calculated labeling ratios between 0.6 and 1.0 label per protein.

Fluorescence spectroscopy: Fluorescence emission spectra were recorded with sample solutions in quartz cuvettes (104F-QS, Hellma, Mühlheim, Germany) by using a QuantaMaster spectrofluorometer (QM-7) from Photon Technology International (Lawrenceville, NJ, USA). The instrument was equipped with a pair of Glan-Thomson polarizers and with a long-wavelength-sensitive photomultiplier (R928, Hamamatsu) to measure dyes emitting in the far red. The unfolding and refolding transitions of PGK (in 30 mM Mops, 50 mM NaCl, 2 mM EDTA, pH 7.4; 0.05–0.1 mg mL^{-1} protein) were monitored by measuring the emission wavelength (λ_{max}) of the intrinsic Trp fluorescence (see, for example, ref. [30]). The excitation wavelength was 295 nm, and all emission spectra (recorded between 300–450 nm) were corrected for background intensities as measured with pure buffer solutions. In addition, Atto655 and Alexa633 emission intensities were measured, in some cases, by using the polarizers to obtain steady-state anisotropy values. For measurements with polymerosomes, the elastic scattering was fitted and thereafter subtracted from the measured emission spectra.

Preparation of polymerosomes and protein encapsulation: The synthesis of ABA triblock copolymers used to form polymerosomes is described elsewhere.[39] The ABA polymer consists of a larger hydrophobic block B (PDMS, with 60 dimethylsiloxane units) and two shorter hydrophilic blocks A (PMOXA, with 20 methyloxazoline units; ABA: $PMOXA_{20}$-$PDMS_{60}$-$PMOXA_{20}$). For polymerosome preparation, 3.6 mg of triblock copolymer and 0.4 mg biotinylated triblock copolymer was dissolved in 1 mL of chloroform. While this solution was permanently rotated in a glass tube, the solvent was evaporated under a nitrogen atmosphere. Subsequently, buffer (0.8 mL, 10 mM Mops, 50 mM NaCl, 2 mM EDTA, pH 7.4) was added dropwise to the dried polymer film. After 20 min of incubation, the solution was sonicated for about 60 s, and 0.2 mL of protein solution (protein concentration in 1 mL of buffer was 0.2–10 μM) was added. Thereafter, this mixture was stirred for periods between 4 and 12 h at room temperature, depending on the protein in use. Typically, the solution became much more transparent after stirring. The resulting suspension was subsequently extruded approximately 20 times through a polycarbonate membrane (diameter 100 nm) using a Lipofast-basic extruder (Avestin Europe GmbH, Mannheim, Germany). In order to remove free (unencapsulated) protein from the monodisperse polymerosomes, the solution was purified using a Sephadex G-75 column (30 cm, MWCO 80 kDa). The obtained elution fractions were measured in a DynaPro dynamic light scattering system from ProteinSolutions (Lakewood, NJ, USA) to determine the amount and size distribution of the polymerosomes. Fluorescence spectroscopy was employed to measure the amount of labeled protein. The polymerosomes obtained were stable and intact for at least several months.

Preparation of slides and immobilization of polymerosomes: Glass slides were cleaned with a PDC-32G plasma cleaner (Harrick Plasma, Ithaca, NY, USA). Poly(ethylene oxide) (PEO) surfaces were formed according to Groll and co-workers.[40] A commercial aminosilane, Vectabond (Vector Laboratories, Burlingame, CA), was used to amino-functionalize the glass slides. PEO (50 mg mL^{-1}) solutions in 50 mM Na_2CO_3 buffer (pH 8) were prepared from mPEG-SPA (M_W 5000, Nektar Therapeutics, Huntsville, AL) or a mixture of biotin-PEG-NHS (50 ng mL^{-1}, M_W 3400, Nektar Therapeutics, Huntsville, AL) and mPEG-SPA (M_W 5000) in a $1:10^6$ ratio. PEO was allowed to react with the Vectabond amino-functionalized surface for 3 h in the dark. Surfaces were washed with Millipore water and were subsequently exposed to streptavidin (2 μg mL^{-1}; Sigma–Aldrich) in the same buffer for 10 min. Finally, the surfaces were incubated with a 1000-fold diluted elution fraction of biotinylated polymerosomes. After 15 min, unbound polymerosomes were washed away with buffer. The streptavidin-biotin binding assay is known to maintain its structural integrity even under strong denaturation conditions.[41]

Confocal microscopy: Time-resolved fluorescence anisotropy decays were measured on a home-built confocal microscope. A droplet of protein or polymerosome-encapsulated protein solution (both at approximately 0.1 μM of protein) was deposited on the surface of a cover slide. The excitation light (640 nm) from a pulsed diode laser (LDH-D-C-640, PicoQuant, Berlin) with a 20 MHz repetition rate was focused by an oil-immersion objective (Apoplan 1.4 N.A./×60, Olympus) onto the buffer solution at approximately 20 μm away from the surface of the cover slide. The fluorescence

emission was collected by the same objective, passed through a dichroic mirror (660DRLP, Omega optical Inc., USA) and focused through a pinhole (100 μm). Subsequently, the emission light was split up by a polarizing beamsplitter cube (Linos Photonics, Göttingen, Germany) and refocused through appropriate emission filters (690DF40) onto single-photon-counting avalanche photodiodes (Perkin–Elmer). The signal was processed by a PicoHarp 300 (PicoQuant, Berlin) TCSPC. electronics board, and the data were analyzed and displayed with custom routines in Matlab.

Wide-field fluorescence microscopy: Individual, surface-tethered polymerosomes containing fluorescently labeled proteins were imaged employing an inverted microscope (Olympus IX-71) in wide-field illumination mode. Excitation light at 640 nm was provided by an argon ion, laser-pumped, dye laser. This light was reflected by a dichroic mirror (Q660 LP, Chroma Technology, Rockingham, VT, USA) into the high numerical aperture objective. Fluorescence emission light was collected by an UPlan 1.3 N.A./×100 oil-immersion objective (Olympus), passed through a discriminating filter (690DF40, Omega Optical), and imaged onto a high-sensitivity Peltier-cooled CCD camera (iXon DV885, Andor Technology, South Windsor, CT, USA). The properties of encapsulated proteins were monitored in situ using a confocal imaging chamber (RC-30HV from Havard Apparatus, Holliston, MA, USA) which enabled us to incubate the polymerosomes with different buffers. The closed chamber was formed by a slotted silicon gasket (5×35 mm) sandwiched between two cover slides. The buffer in the chamber (50 μL) was exchanged using a syringe connected to the chamber via two peripheral tubings (the required time for buffer exchange was approximately 15 s). To evaluate integrated intensities from individual spots, the images were processed with custom-written Matlab routines.

Anisotropy measurements: For anisotropy measurements, linearly polarized light (either vertically or horizontally polarized) was used to excite fluorophores in solution, and the fluorescence emission was measured for vertical and horizontal polarizer orientations ($I_\perp$ and $I_\parallel$). Fluorescence anisotropy is defined as:

$$r = \frac{(I_\parallel/I_\perp)-1}{(I_\parallel/I_\perp)+2} \quad (1)$$

For steady-state anisotropies, a single channel (L-format) configuration was used, and we performed four individual measurements, which gave us the required anisotropy [Equation (2)]:

$$r = \frac{I_{VV}-GI_{VH}}{I_{VV}+2GI_{VH}} \text{ with } G = \frac{I_{HV}}{I_{HH}} \quad (2)$$

Here the *G* factor corrects for the different detection efficiencies of the horizontal and vertical emission pathways. In anisotropy decay measurements, a two channel (T-Format) configuration was employed, where the vertical and horizontal emission components are detected simultaneously. By using vertically and horizontally polarized excitation light, the anisotropy can be calculated as given by Equation (1) (for details see ref. [33]).

Abbreviations

BLA: *Bac. licheniformis* α-amylase, DLS: dynamic light scattering, DMPC: 1,2-dimyristoyl-*sn*-glycero-3-phosphocholine, DOPE: L-α-dioleoyl phosphatidylethanolamine, EDTA: ethylenediaminetetraacetic acid, EggPC: L-α-phosphatidylcholine, hydrogenated (egg, chicken), FCS: fluorescence correlation spectroscopy, GdnHCl: guanidine hydrochloride, Mops: 3-(*N*-morpholino)propanesulfonic acid, PDMS: poly-dimethylsiloxane, MWCO: molecular weight cut off, PET: photoinduced electron transfer, PMOXA: polymethyloxazoline, POPC: 1-palmitoyl-2-oleoyl-*sn*-glycero-3-phosphocholine, PGK: phosphoglycerate kinase, TCSPC: time-correlated single-photon counting.

Acknowledgements

Jürgen Groll (SusTech GmbH & Co KG, Darmstadt) is greatly acknowledged for providing us with a protocol for cover slide coatings. We thank Iris v. d. Hocht for providing Atto655-labeled DOPE. T.R. acknowledges financial support by the International Helmholtz Research School on Biophysics and Soft Matter ("BioSoft"). J.F. thanks G. Büldt (Forschungszentrum Jülich) for continuous and sustainable support in his institute.

Keywords: fluorescence spectroscopy · photoinduced electron transfer · protein encapsulation · protein folding · single-molecule studies

[1] T. D. Heath, R. T. Fraley, D. Papahdjopoulos, *Science* **1980**, *210*, 539–541.
[2] J. N. Weinstein, L. D. Leserman, *Pharmacol. Ther.* **1984**, *24*, 207–233.
[3] R. C. Dutta, *Curr. Pharm. Des.* **2007**, *13*, 761–769.
[4] D. K. Eggers, J. S. Valentine, *J. Mol. Biol.* **2001**, *314*, 911–922.
[5] D. K. Eggers, J. S. Valentine, *Protein Sci.* **2001**, *10*, 250–261.
[6] B. Okumus, T. J. Wilson, D. M. Lilley, T. Ha, *Biophys. J.* **2004**, *87*, 2798–2806.
[7] M. Kumar, M. Grzelakowski, J. Zilles, M. Clark, W. Meier, *Proc. Natl. Acad. Sci. USA* **2007**, *104*, 20719–20724.
[8] M. Nasseau, Y. Boublik, W. Meier, M. Winterhalter, D. Fournier, *Biotechnol. Bioeng.* **2001**, *75*, 615–618.
[9] I. Shin, E. Wachtel, E Roth, C. Bon, I. Silman, L. Weiner, *Protein Sci.* **2002**, *11*, 2022–2032.
[10] D. T. Chiu, C. F. Wilson, A. Karlsson, A. Danielsson, A. Lundqvist, A. Stromberg, F. Ryttsen, M. Davidson, S. Nordholm, O. Orwar, R. N. Zare, *Chem. Phys.* **1999**, *247*, 133–139.
[11] E. Boukobza, A. Sonnenfeld, G. Haran, *J. Phys. Chem. B* **2001**, *105*, 12165–12170.
[12] I. Cisse, B. Okumus, C. Joo, T. Ha, *Proc. Natl. Acad. Sci. USA* **2007**, *104*, 12646–12650.
[13] I. Gill, A. Ballesteros, *Trends Biotechnol.* **2000**, *18*, 282–296.
[14] P. Walde, S. Ichikawa, *Biomol. Eng.* **2001**, *18*, 143–177.
[15] J. P. Colletier, B. Chaize, M. Winterhalter, D. Fournier, *BMC Biotechnol.* **2002**, *2*, 9–17.
[16] B. M. Discher, Y. Y. Won, D. S. Ege, J. C. Lee, F. S. Bates, D. E. Discher, D. A. Hammer, *Science* **1999**, *284*, 1143–1146.
[17] A. Mecke, C. Dittrich, W. Meier, *Soft Matter* **2006**, *2*, 751–759.
[18] X. Michalet, S. Weiss, M. Jager, *Chem. Rev.* **2006**, *106*, 1785–1813.
[19] H. P. Lu, L. Xun, X. S. Xie, *Science* **1998**, *282*, 1877–1882.
[20] E. Rhoades, E. Gussakovsky, G. Haran, *Proc. Natl. Acad. Sci. USA* **2003**, *100*, 3197–3202.
[21] E. V. Kuzmenkina, C. D. Heyes, G. U. Nienhaus, *Proc. Natl. Acad. Sci. USA* **2005**, *102*, 15471–15476.
[22] J. C. M. Lee, H. Bermudez, B. M. Discher, M. A. Sheehan, Y. Y. Won, F. S. Bates, D. E. Discher, *Biotechnol. Bioeng.* **2001**, *73*, 135–145.
[23] P. Rigler, W. Meier, *J. Am. Chem. Soc.* **2006**, *128*, 367–373.
[24] D. E. Discher, A. Eisenberg, *Science* **2002**, *297*, 967–973.
[25] N. Marmé, J.-P. Knemeyer, M. Sauer, J. Wolfrum, *Bioconjugate Chem.* **2003**, *14*, 1133–1139.
[26] H. Neuweiler, S. Doose, M. Sauer, *Proc. Natl. Acad. Sci. USA* **2005**, *102*, 16650–16655.
[27] S. K. Das, M. Darshi, S. Cheley, M. I. Wallace, H. Bayley, *ChemBioChem* **2007**, *8*, 994–999.
[28] C. G. Choquet, G. B. Patel, G. D. Sprott, T. Beveridge, *Appl. Microbiol. Biotechnol.* **1994**, *42*, 375–384.
[29] K. H. Strucksberg, Diploma Thesis, Universität Duesseldorf (Germany), **2007**.

[30] K. H. Strucksberg, T. Rosenkranz, J. Fitter, *Biochim. Biophys. Acta, Proteins Proteomics* **2007**, *1774*, 1591–1603.
[31] S. Paula, A. G. Volkov, A. N. Van Hoek, T. H. Haines, D. W. Deamer, *Biophys. J.* **1996**, *70*, 339–348.
[32] E. Rhoades, M. Cohen, B. Schuler, G. Haran, *J. Am. Chem. Soc.* **2004**, *126*, 14686–14687.
[33] J. R. Lakowicz, *Principles of Fluorescence Spectroscopy*, Kluwer Academic/Plenum, New York, **1999**.
[34] S. Weiss, *Science* **1999**, *283*, 1676–1683.
[35] A. A. Deniz, T. A. Laurence, G. S. Beligere, M. Dahan, A. B. Martin, D. S. Chemla, P. E. Dawson, P. G. Schultz, S. Weiss, *Proc. Natl. Acad. Sci. USA* **2000**, *97*, 5179–5184.
[36] K. Chattopadhyay, S. Saffarian, E. L. Elson, C. Frieden, *Proc. Natl. Acad. Sci. USA* **2002**, *99*, 14171–14176.
[37] S. Doose, H. Neuweiler, M. Sauer, *ChemPhysChem* **2005**, *6*, 2277–2285.
[38] P. Broz, S. Driamov, J. Ziegler, N. Ben Haim, S. Marsch, W. Meier, P. Hunziker, *Nano Lett.* **2006**, *6*, 2349–2353.
[39] C. Nardin, T. Hirt, J. Leukel, W. Meier, *Langmuir* **2000**, *16*, 1035–1041.
[40] J. Groll, E. V. Amirgoulova, T. Ameringer, C. D. Heyes, C. Rocker, G. U. Nienhaus, M. Moller, *J. Am. Chem. Soc.* **2004**, *126*, 4234–4239.
[41] M. González, L. A. Bagatolli, I. Echabe, J. L. R. Arrondo, C. E. Argarana, C. R. Cantor, G. D. Fidelio, *J. Biol. Chem.* **1997**, *272*, 11288–11294.

Received: November 11, 2008
Published online on February 3, 2009

